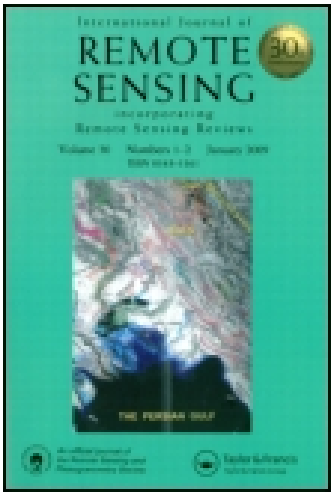


International Journal of Remote Sensing

Publication details, including instructions for authors and subscription information:
http://www.tandfonline.com/loi/tres20

# A temperature-controlled spectrometer system for continuous and unattended measurements of canopy spectral radiance and reflectance

Guillaume Drolet[a], Tom Wade[a], Caroline J. Nichol[a], Chris MacLellan[b], Janne Levula[c], Albert Porcar-Castell[d], Eero Nikinmaa[d] & Timo Vesala[e]

[a] School of GeoSciences, University of Edinburgh, Edinburgh EH9 3JN, UK

[b] NERC Field Spectroscopy Facility, School of GeoSciences, Grant Institute, University of Edinburgh, Edinburgh EH9 3JW, UK

[c] Hyytiälä Forestry Field Station, University of Helskinki, Korkeakoski FI-35500, Finland

[d] Department of Forest Sciences, University of Helsinki, Helsinki FI-00014, Finland

[e] Department of Physics, University of Helsinki, Helsinki FI-00014, Finland

Published online: 21 Feb 2014.

To cite this article: Guillaume Drolet, Tom Wade, Caroline J. Nichol, Chris MacLellan, Janne Levula, Albert Porcar-Castell, Eero Nikinmaa & Timo Vesala (2014) A temperature-controlled spectrometer system for continuous and unattended measurements of canopy spectral radiance and reflectance, International Journal of Remote Sensing, 35:5, 1769-1785, DOI: 10.1080/01431161.2014.882035

To link to this article: http://dx.doi.org/10.1080/01431161.2014.882035

*International Journal of Remote Sensing*, 2014
Vol. 35, No. 5, 1769–1785, http://dx.doi.org/10.1080/01431161.2014.882035

Taylor & Francis
Taylor & Francis Group



# TECHNICAL NOTE

# A temperature-controlled spectrometer system for continuous and unattended measurements of canopy spectral radiance and reflectance

Guillaume Drolet[a]*, Tom Wade[a], Caroline J. Nichol[a], Chris MacLellan[b], Janne Levula[c], Albert Porcar-Castell[d], Eero Nikinmaa[d], and Timo Vesala[e]

[a]*School of GeoSciences, University of Edinburgh, Edinburgh EH9 3JN, UK;* [b]*NERC Field Spectroscopy Facility, School of GeoSciences, Grant Institute, University of Edinburgh, Edinburgh EH9 3JW, UK;* [c]*Hyytiälä Forestry Field Station, University of Helskinki, Korkeakoski FI-35500, Finland;* [d]*Department of Forest Sciences, University of Helsinki, Helsinki FI-00014, Finland;* [e]*Department of Physics, University of Helsinki, Helsinki FI-00014, Finland*

(*Received 1 October 2013; accepted 19 December 2013*)

This paper describes the development of a fully automated system for collecting high-resolution spectral data over a forested footprint. The system comprises a pair of off-the-shelf spectrometers in a custom-built thermal enclosure with a fixed off-nadir downward (target)-pointing fibre and upward-pointing fibre for irradiance measurement. Both instruments sample simultaneously via custom-written and user-controlled software during all weathers and sky conditions. The system is mounted on a 25 m eddy covariance scaffolding tower, approximately 7 m from a Scots pine forest canopy. The system was installed at the University of Helsinki's SMEAR-II Field Station in Hyytiälä in March 2010 and has been operating continuously through a joint programme between the Universities of Edinburgh and Helsinki. The system was designed to capture diurnal and seasonal variation in vegetation light-use efficiency and fluorescence through the capture and analysis of well-defined narrow spectral features, but its implementation would permit the extraction of further optical signals linked to vegetation biophysical variables, and provide a continuous data stream with which to validate satellite data products including vegetation indices such as the photochemical reflectance index (PRI) as well as spectral indicators of solar induced fluorescence.

## 1. Introduction

Photosynthesis, the light-driven conversion by plants of atmospheric carbon dioxide ($CO_2$) into water vapour and oxygen, is one of the most important natural processes on Earth. As one of the largest sinks for $CO_2$, vegetation photosynthesis plays a key role in determining the global carbon (C) balance (Valentini et al. 2000). However, because plants are highly adapted organisms and can quickly respond to changes in their environment, the amount of carbon they can remove from the atmosphere is highly dependent on the environmental conditions in which they thrive, thus making it difficult to predict (IPCC 2007). Because of its high significance to the global C budget and its high variability, the ability to monitor photosynthetic C uptake globally has become of major interest to both the carbon-cycle science and remote-sensing communities, but also to decision-makers interested in climate mitigation scenarios or targets in reduction of fossil fuel emissions (IPCC 2007). Currently, two main approaches exist to estimate

*Corresponding author. Email: guillaume.drolet@mrn.gouv.qc.ca

photosynthesis directly from remotely sensed measurements. The first is based on measurements of the photochemical reflectance index (PRI), a numerical index that uses the spectral reflectance values measured in a narrow detection band at 531 nm and in a reference band at 570 nm (Gamon et al. 1992). This index is related to the amount of absorbed energy in the leaf that is directed to non-photochemical quenching (NPQ), a process by which plants thermally dissipate excessive energy under sub-optimal photosynthetic conditions (Demmig-Adams and Adams 1996; Demmig-Adams 1998). During that process, xanthophyll pigments in the chloroplast undergo reversible or sustained changes through de-epoxidation of violaxanthin into zeaxanthin, resulting in changes in leaf level reflectance at 531 nm, which can in turn be related to the level of photosynthesis down-regulation at the canopy level (Demmig-Adams and Adams 1996; Demmig-Adams 1998). The second approach to estimating photosynthesis from remotely sensed measurements is based on a phenomenon called chlorophyll fluorescence ($F$). $F$ is the re-emission of photons at longer wavelengths (i.e. lower energy) than those at which they were absorbed. When actively photosynthesizing, plants continuously re-emit a small fraction of the absorbed energy from photosynthesis to $F$, which fluctuates in response to changes in environmental conditions. It is possible to directly measure variations in $F$ using radiometric measurements in very narrow wavebands and using appropriate algorithms (e.g. Fraunhofer Line Discriminator, Spectral Fitting), or indirectly by using spectral indices calculated from the reflectance measured at wavelengths related to changes in $F$ (Plascyk 1975; Plascyk and Gabriel 1975; Alonso et al. 2008; Maier et al. 2003; Meroni and Columbo 2006; Moya et al. 2006; Meroni et al. 2009). Because NPQ and $F$ are closely linked to photosynthetic efficiency, an increase in the amount of energy directed to any of these three processes will unavoidably lead to a decrease in energy available for the other two. Therefore, if we can accurately estimate $F$ and NPQ it is then possible to have a measure of the level of efficiency of carbon uptake by plants.

Although both the PRI- and $F$-based approaches were successfully applied at the plant and small canopy levels (Campbell et al. 2007, 2008), their application to larger spatial scales using airborne and satellite data remains challenging (Joiner et al. 2011, 2012; Frankenburg et al. 2012; Guanter et al. 2012). PRI is known to have an anisotropic response (i.e. it is a function of the sun-observation geometry) (Hilker et al. 2008, 2009) and its measurement from airborne or spaceborne platforms is also affected by atmospheric effects (Drolet et al. 2005, 2008; Hilker et al. 2011). Similarly, remote sensing of $F$ is difficult because of the very small amount of energy naturally emitted by chlorophyll, which depends not only on the environment of the plant but also on the leaf or canopy chlorophyll content and on the amount of energy directed to NPQ relative to $F$ (Adams et al. 1990; Logan et al. 2007). Therefore, before we can routinely apply these methods at regional scales and to temporally sparse data, as is usually the case with data from space-based platforms, we need a very detailed understanding of all the processes affecting the upscaling of these complex and small signals.

The use of field spectrometers for continuous measurements of plant spectral properties has increased in popularity over the past few years (Hilker et al. 2007; Meroni et al. 2011). This accrued interest in field spectrometry is partly explained by the recent advent of a range of compact instruments allowing for the measurement, with a high level of accuracy and precision, of subtle changes in plant spectral properties that can be related to changes in plant functioning. This growing interest in field spectrometry is mostly driven by the previously mentioned need to improve the models and algorithms that can be used to scale these important physiological processes from canopies up to landscapes and continents (Hall et al. 2011; Hilker et al. 2011). A characteristic common to most of

these field instruments is the availability of several contiguous and very narrow wavebands (e.g. sub-nanometre spectral resolution) in regions of the electromagnetic spectrum associated with important physiology-related processes. However, these portable instruments, unless modified in some way, are not well suited for measuring the short- and long-term changes in physiological properties associated with PRI and *F*. First, most commercially available instruments have been designed for periodic use whereas improvement of remote-sensing methods for *F* and PRI needs *continuous* measurements under a wide range of environmental conditions, which usually span multiple seasons or years. In doing so, the measurements can be used not only for diurnal responses but also those at the interannual time scale. Secondly, all field spectrometers need to be temperature-stabilized as a lack of thermal stability results in drift both in wavelength position and radiometric response. Such control however necessitates more power than is usually possible for continuous field measurements using battery-based systems. Finally, the current cost for the available field instruments still remains prohibitive, in part due to temperature-stabilizing systems inside these instruments. Here, we developed a custom-built, low-cost, low-power system that meets the requirements for remote sensing of vegetation at narrow wavelengths and is therefore highly applicable for both PRI and *F* and can be easily deployed to different study sites. In this paper we present the design and performance of the system, followed by preliminary results from a ground-level study. We finally discuss how this system could be extended to airborne measurements.



## 2. System requirements and conception

### 2.1. Measurement requirements

To better understand how spectral signals scale across space and time requires continuous measurements of both the downwelling solar irradiance and the upwelling radiance reflected by the canopy in regions of the electromagnetic (EM) spectrum specific to the processes under study. For studies of PRI and *F* in particular, this region encompasses parts of the visible (500–700 nm) and the near-infrared (700–900 nm) and must include narrow wavebands at 531, 550, 570, 687, and 760 nm. More specifically, *F* extraction techniques based on the Fraunhofer lines require the simultaneous measurement of both the radiance reflected by the canopy and the solar downwelling irradiance at two wavebands closely located on the EM spectrum. One is a detection band sitting inside an atmospheric molecular absorption feature (e.g. oxygen at 687 nm; $O_A$-B) and the other a reference band located on the shoulder of that feature. Moreover, the spectral resolution requirements for *F* studies using passive sensors are generally in the order of subnanometres to only a few nanometres (Meroni et al. 2009). For PRI studies, the required full width at half maximum (FWHM) for both the detection and reference band is around 10 nm (Gamon et al. 1992).

Because of its relatively low cost and compact size, and the possibility of having the instrument custom-built according to a project's spectral and radiometric requirements, we developed our system around a pair of commercially available Ocean Optics USB2000+ spectrometers (http://www.oceanoptics.com) that were custom-built according to our specifications with full technical details outlined in Table 1.

We opted for a dual-beam system configuration, in which downwelling solar irradiance and reflected radiance measurements are acquired simultaneously by each instrument, as opposed to a single-beam configuration. In the latter configuration, the reference panel and target canopy are measured sequentially by a single instrument, thus increasing

Table 1. Technical specifications of the Ocean Optics USB-2000+ spectrometers.

| Parameter | Description | Values |
|---|---|---|
| Integration time | Time duration (ms) of each measurement | Instrument dependent. USB2000 + : minimum 1 ms, maximum 60 s |
| Auto-optimize | If checked, entered integration time is ignored and rather is adjusted before each measurement to account for illumination conditions | Yes/No |
| Acquisition frequency | Measurement repeat interval (min) | 1, 2, 5, 10, 15, 20, 30, 60 |
| Acquisition period | Determines whether measurements occur all day long or during a daily time window only | Continuous (5 am–6 pm local time) or fixed period (between StartHour and StopHour) |
| Scans to average | Number of spectra to average for each recorded spectrum (total acquisition time = (integration time) × (scans to average) | Integers between 1 and 250 |
| Boxcar width | Width (pixels) of an averaging window that can be used for smoothing spectra to reduce noise | Integers between 1 and 250 |
| Nonlinearity correction | Option for correcting for nonlinearity response of the detectors | Yes/No |
| Electric dark correction | Option for subtracting optically dark detectors to remove the noise baseline from spectra | Yes/No |
| Dark spectrum acquisition time | Time for acquiring a dark spectrum | Between 1 am and 4 am (local time). Default 2 am |
| Triggering mode | Option for starting a measurement | Normal/Software/Synchronization/ External Hardware. Only Normal and External Hardware currently implemented |



the possibility of changes in atmospheric and illumination conditions between the two measurements. This possibility is eliminated in a dual-beam configuration (Rollin et al. 1998; Balzarolo et al. 2011). In our system, the upward-pointing optical fibre of one spectrometer is fitted with a cosine corrector (CC-3, Ocean Optics) for measuring downwelling solar irradiance. The second spectrometer measures reflected radiance with an optical fibre pointed at the canopy and can also be fitted with a fore-optic to restrict its field-of-view.

The area of the canopy viewed by the sensor and from which reflected radiance is measured (i.e. the footprint) can be adjusted in different ways. First, the location of the footprint can be moved across the canopy by rotating the target-pointing optical fibre about a vertical axis such as a metal rod fastened to the top platform of a scaffolding tower (Figure 1). Second, it is possible to reduce or increase the footprint size by sliding the optical fibre up or down along the axis or by changing the observation angle of the fibre relative to nadir. Finally, the size of the footprint can also be modified by fitting the target fibre with a fore optic lens. Finally, for most studies of PRI or *F*, the azimuth and zenith angles of the target-pointing fibre should be set in a direction which will maximize the amount of reflected radiance measured by the spectrometer. This is required for obtaining the largest signal-to-noise possible but it is also, in these viewing conditions, close to the

backscattering direction (i.e. maximum light reflected from the sun in the field-of-view) from which most of the structure- and physiology-related information will be extracted (Hall et al. 2008; Hilker et al. 2008).

Another critical requirement for remote sensing of plant physiological signals is a measurement frequency that is in agreement with the fast and/or slow processes that are occurring in the leaves. For example, variations in the overall levels of xanthophyll cycle pigments occur slowly in response to seasonal changes in light and temperature (i.e. sustained thermal dissipation) (Porcar Castell et al. 2008). On the other hand, these same pigments can quickly change conformation (violaxanthin→zeaxanthin) in response to excessive incoming radiation (i.e. flexible thermal dissipation), and this rapidly occurring conversion will restore prior levels of violaxanthin and zeaxanthin in the order of minutes to hours after illumination conditions have returned to less stressful levels (Demmig-Adams and Adams 2006). To capture the changes in radiometric signals that are associated with such pigment conversions, it is necessary to have a system which offers the possibility of acquiring spectra at fast and high-repeat intervals, depending on the processes being studied.

### 2.2. *System components and design*

One of the main objectives in designing this system was that it could be left alone in the field for prolonged periods yet still be able to collect reliable data at user-defined intervals. Field spectrometers need to be temperature stabilized as a number of their component electronics or optical parts are affected by temperature changes, which results in unreliable calibration parameters and often unquantifiable reduction in the quality of the data they produce. For example, the specification of the Sony ILX511 2048-element linear silicon CCD array detector fitted to USB 2000+ spectrometers indicates that two major components of the 'Dark Signal', the offset level voltage and the dark voltage rate, have positive thermal gradients (www.oceanoptics.com/technical/detectorsonyILX511.pdf). In addition to this, it has to be assumed that the spectral sensitivity of the silicon detector will have temperature dependencies, especially in the near-infrared region close to the band gap. For a typical silicon photodiode, this can be as high as 0.1% $°C^{-1}$ at 1000 nm and 0.5% $°C^{-1}$ at 1050 nm (Hartmann et al. 2001). For this reason, many spectrometer systems include heaters and/or coolers to maintain constant temperature during operation. For example, the HR-1024 instrument (Spectra Vista Corporation, Poughkeepsie, NY, USA) uses a heater to maintain the temperature of its visible-near-infrared (VNIR) photodiode array at 40°C while thermoelectric cooling is used to maintain the temperature of its shortwave infra-red InGaAs detector arrays (SWIR 1 and 2) at 0 and –5°C, respectively. Similarly, the FieldSpec Pro spectrometer (Analytical Spectral Devices, Boulder, CO, USA) also uses thermoelectric cooling to control the temperature of its SWIR 1 and 2 InGaAs detectors. Coolers are energy-hungry and thus to reduce the system's energy consumption to a minimum, we decided to exclude coolers from our design. Instead, we rely only on heat loss for cooling. The two spectrometers are located inside a small plastic insulated enclosure (Figure 2). Insulation is achieved by lining the inside of the enclosure with pieces of 1″ urethane insulated panels; 5 and 10 W self-adhesive heater mats (RS Electronics, UK) are attached to the back of an aluminium plate at the bottom of the enclosure, which also holds the support for the spectrometers, a fan to distribute the heat, a heat sink (model ZM-NBF47, Zalman Tech Co., Ltd., Seoul, Korea), and copper strips connecting the heat sink to the spectrometers. A resistance temperature detector (RTD) element is located directly under the spectrometers and is connected to a temperature

Figure 1. The spectrometer system is mounted on a metal rod at the top of a scaffolding tower. The target-looking fibre can be slid up or down and rotated around the rod to change the measurement footprint size and location.

controller (CN132-24V, Omega Engineering Ltd, UK) located outside the small enclosure but inside a larger, non-insulated enclosure (Figure 3). The temperature controller starts and stops the heater mats and the fan when the temperature drops below a set point. Heat

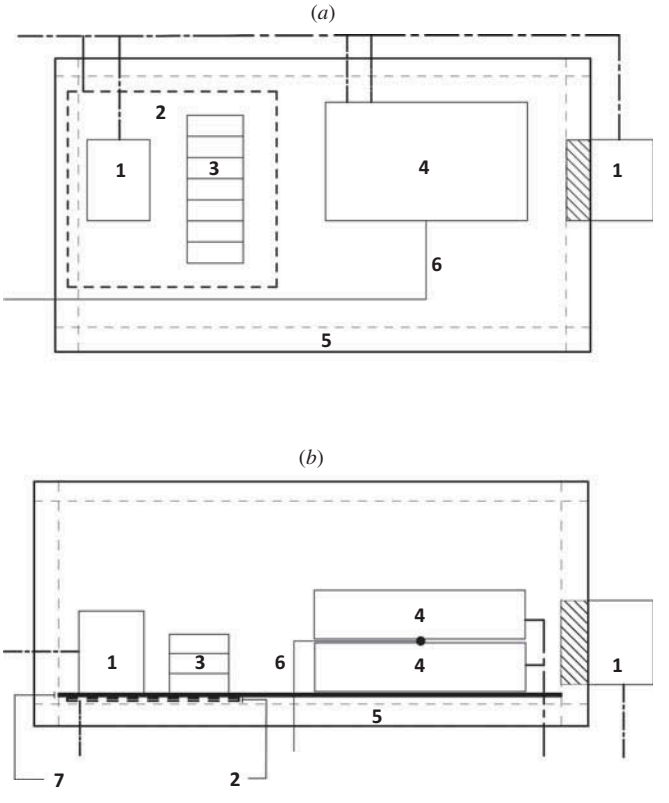


Figure 2. Top (*a*) and side (*b*) views of the inner enclosure showing: (1) fans, (2) heater mats, (3) heat sink, (4) spectrometers, (5) insulated panels, (6) temperature detector, and (7) aluminium plate. Drawings are not to scale.

is lost from imperfect insulation and also from a thick piece of aluminium intersecting one of the enclosure walls and connected to another heat sink outside the enclosure. During hot summers, a piece of insulation board is removed from one of the walls of the spectrometer enclosure and is replaced with an extractor fan that is also connected to the temperature controller and started when the temperature rises above a second set point.

The spectrometer enclosure is attached to a metal frame inside a larger enclosure which also houses the temperature controller, a notebook to operate the spectrometers and for recording the data, a stabilised-output PSR 230 primary switched-mode power supply (Block Transformatoren-Elektronic GmbH & Co.KG, Verden, Germany) used as an AC to DC converter when required, and Drierite® $CaSO_4$ dessicant bags (Drierite, Xenia, OH) to remove extra moisture from the enclosures (Figure 3). Heat from the small enclosure is dissipated out of the larger enclosure through holes drilled in the sides of the large enclosure. During summer, a continuously running extractor fan is added to help in dissipating heat from the large enclosure. Finally, the outside of the large enclosure is covered with insulating reflecting material. If the system is operated during colder months, a second layer of insulating material is also added.

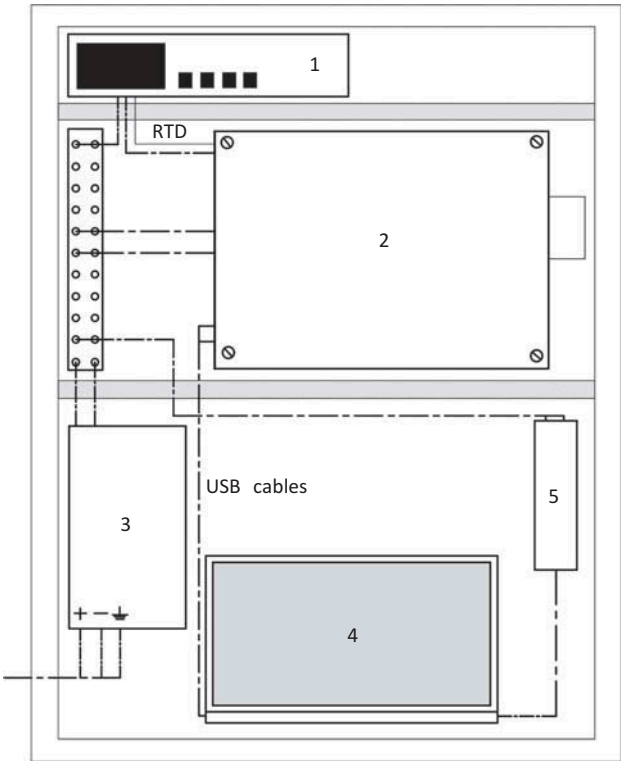


Figure 3. Front view of the outer enclosure showing: (1) the temperature controller, (2) the inner enclosure, (3) the AC–DC power converter, (4) notebook, and (5) notebook charger. Drawings are not to scale.

### 2.3. *Software*

Spectrum acquisition is controlled by a program running on the notebook located inside the large enclosure. SpectraSuite is the standard platform for operating the range of Ocean Optics spectrometers. For our system we used OmniDriver, a development tool from Ocean Optics which allows for control of spectrometers within custom application software. OmniDriver is available for many programming languages. We used the Java language to develop our software, which we call 'OO Controller'. The program is platform-independent and runs as a graphical user interface (GUI) that allows the setting of most of the acquisition parameters needed for making continuous measurements (Table 2).

Among the many OO Controller features, the 'Auto-Optimize' feature is one of the most important for continuous measurement in a variable light environment. The 'Auto-Optimize' function allows maximization of measurement signal-to-noise ratio by determining the integration time values that will yield spectra maximum values of about 85% of the detector's range before saturation. This is done by acquiring, just before each acquisition and for each instrument, two spectra at different integration times. Assuming a linear response of the detectors with time, a linear regression equation is derived using the change in intensity count, for the detector element which records the spectrum maximum value, as a function of integration time. This equation is then used to estimate the optimized integration times for each instrument.

Table 2. List of Ocean Optics spectrometer controller acquisition parameters.

| Parameter | Performance |
|---|---|
| Sensor | 350–1000 nm |
| Resolution | FWHM 1 nm (0.3 nm interval) |
| Integration time | 1 ms to 65 s |
| Power up time | ~2 s |
| Power requirement | 250 mA at +5 VDC |
| Supply voltage | 4.5–5.5 V |
| Detector | Sony ILX511B CCD |
| Signal to noise | 250:1 single acquisition |
| Operation temperature | −10° to +50°C |
| Operation humidity | 0% to 90% non-condensing |
| Interfaces | USB 2.0, 480 Mbps 2-wire RS-232 |



To obtain concomitant measurements from both spectrometers, total measurement periods (integration time × number of averaged spectra) are first calculated for each instrument to determine the one that will take the longest to complete. At the time of measurement, the instrument with the longest acquisition time will start first, followed shortly by the second instrument. The time delay between the start of the first and second instruments is determined so that the half-points of the total acquisition times of both instruments match.

Diagnostic plots are another important feature of the OO Controller. These plots are accessible from the menu bar and allow viewing, for each instrument, of the spectra from the previous five acquisitions (Figure 4). The plotted spectra are in units of intensity count. This feature is critical for checking that measurements are performing as intended before leaving the site until the next calibration or maintenance visit.

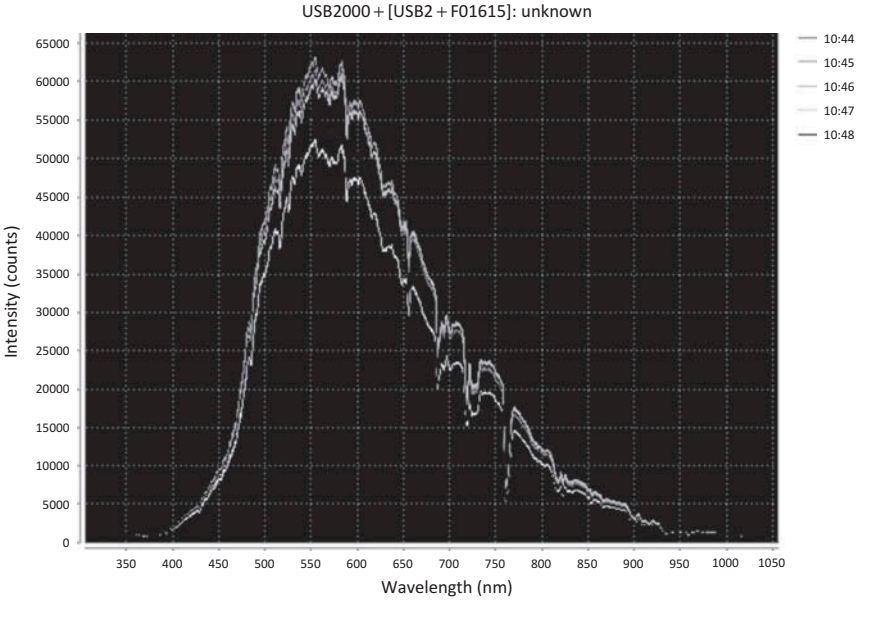


Figure 4. Screen capture of the diagnostic plot window showing the last five raw and unprocessed spectra from a single instrument connected to the system. The software can display two spectrometers side by side in real time in this window.

When making continuous measurements in remote areas such as forests, there is a risk of missing critical data during periods of interest because of malfunction in the system components. The length of potential gaps in the data time series increases with the interval between each visit to the measurement site. To reduce the risk of extended periods with missing data that could result from software malfunction, we scheduled a daily task on the notebook operating system that reboots the computer every 24 h at midnight. At start up, a second scheduled task initiates the OO Controller which will resume acquisition using the previously used settings.

## 3. Results

The system was deployed at the top of a scaffolding eddy covariance flux tower at the University of Helsinki's SMEAR-II research station (Hari and Kulmala 2005) in Hyytiälä, Southern Finland in March 2010. The canopy-pointing optical fibre was placed at a distance of 7 m above the canopy. At this height, the 24.8° field-of-view (FOV) of the optical fibre yielded an off-nadir instantaneous FOV of approximately 400 $m^2$ on the canopy (Figure 5). The azimuth angle of the fibre was 280° and its viewing angle was about 70° relative to nadir. The azimuth angle of 280° allowed observation of mostly sunlit trees during daytime when the sun was higher than 35° above the horizon. In this study we used 2 m-long premium-grade shielded 600 µm optical fibre for both spectrometers. It is well documented that attenuation in the measurement of signal-to-noise ratio increases with optical fibre length, and this attenuation is wavelength- and fibre-dependent (http://www.oceanoptics.com/Products/fiberattenuation.asp). Given the average signal-to-noise ratio of our measurements over a boreal forest target, we decided that a fibre length of 2 m was desirable to ensure reliable signal strength and functionality. Because the fibres are attached to the spectrometers inside the enclosure, this prevented us from mounting the system higher above the canopy to obtain a larger footprint size, but the whole system itself could be mounted on a higher platform if an increase in footprint size is required.

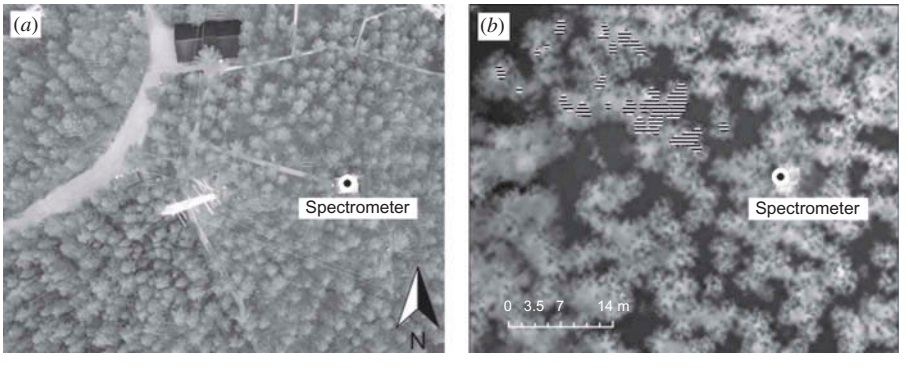


Figure 5. (*a*) Aerial photography of the Hyytiälä field station flux tower and location of the spectral system on the scaffolding tower. (*b*) Approximate location and size of the instantaneous field-of-view of the downward-looking optical fibre (black and white stripes). The system is viewing several tree crowns. The greyscale image is a canopy surface model derived from an airborne lidar acquisition. The FOV was modelled as a square-based pyramid having its apex at the location of the spectrometer system, with a 25° vertex angle, looking in the same direction as the canopy-pointing fibre.

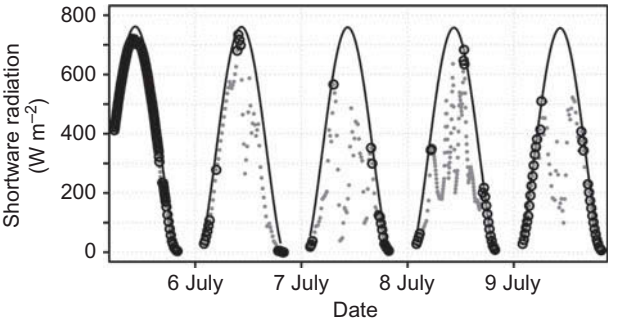


Figure 6. Shortwave radiation measurements, model predictions, and cloud flag. The solid black line is the simulated potential shortwave radiation, grey dots are radiation measurements measured at the flux tower, and black circles are observations identified as 'clear' based on the absolute differences between simulations and observations.



Low levels of incoming radiation during winter months at the latitude of the study site prevent the acquisition of useable spectral measurements with our system. For the first measurement season (May–September 2010), the system was programmed to acquire one scan (i.e. simultaneous irradiance and radiance spectra) every 15 minutes between 8:00 and 16:00 (local time). To determine sky conditions at times of acquisition, we used near-simultaneous radiation measurements from sensors located on the same tower as our system, which we compared with radiation predictions from a model (Linacre 1992). Based on arbitrary thresholds in the difference between radiation measurements and model predictions, we created three classes of sky conditions (Clear, Possibly Cloudy, Cloudy) to help in interpreting the spectrometer data (Figure 6).

During the months of July and August 2010, the optical bench temperatures of the spectrometers varied between 42.8°C and 44.4°C (mean = 43.4°C, 3.4°C above the system set point at 40°C) with a few peaks about 0.5 to 1.0°C above the mean on exceptionally warm days (Figure 7). For that same period, the mean temperature outside the enclosure varied between 5.8°C and 32.4°C, with a mean of 17.8°C (Figure 7).

To convert the measured spectra from intensity counts to physical units of radiance (mW cm$^{-2}$ sr$^{-1}$ nm$^{-1}$) and irradiance (mW cm$^{-2}$ nm$^{-1}$) (Figure 8), and to keep track of the system's radiometric performance, regular radiometric calibrations need to be carried through. Over the period between March 2010 to March 2011 we performed

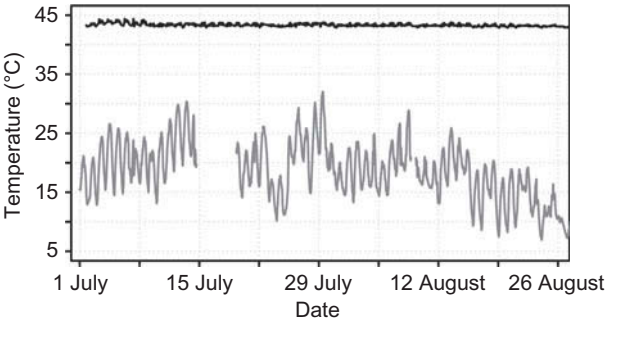


Figure 7. Spectrometer optical bench temperature (black line) and air temperature measured at 16 m above the canopy (grey line) for July and August 2010.

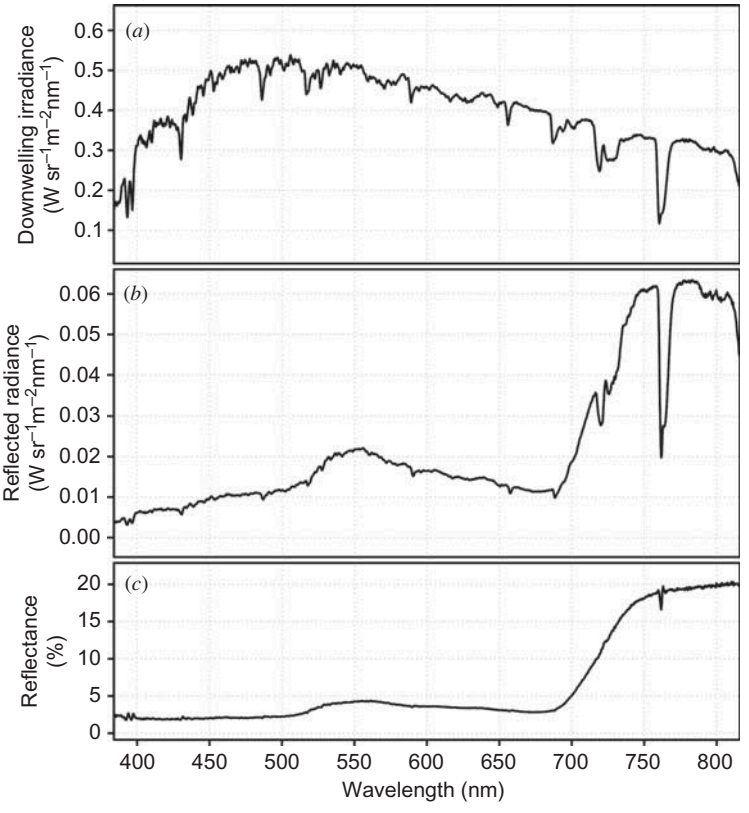


Figure 8. Calibrated spectra for (*a*) downwelling irradiance, (*b*) reflected radiance and (*c*) reflectance from measurements taken on 6 July 2011 at 8:15 (UTC) at the Hyytiälä field station, Finland.

a set of six wavelength and radiometric calibrations of the spectrometers, with the radiometric stability of the system being assessed by cross-comparing the calibration curves from each calibration. For a given measurement period between two calibrations, we utilized the calibration curves from the first radiometric calibration at the beginning of the period to convert the spectra to radiance and irradiance units. It could be argued that for long measurement periods, a calibration curve closest in time to the measurements would be better suited than that acquired at the beginning of the period. Figure 8 shows an example of calibrated spectra for radiance and irradiance measurements. The irradiance as measured with the cosine diffuser represents the integration of the directional irradiance ($sr^{-1}$) over the hemisphere above it. Although the angular response of the diffuser is not perfectly lambertian, we assumed it is and calculated spectral reflectance $\rho(\lambda)$ as

$$\rho(\lambda) = \frac{L(\lambda)}{E(\lambda)}\,\pi, \tag{1}$$

where $L(\lambda)$ is reflected spectral radiance (mW cm$^{-2}$ nm$^{-1}$ sr$^{-1}$) at wavelength $\lambda$ and $E$ ($\lambda$) is downwelling solar irradiance (mW cm$^{-2}$ nm$^{-1}$) at wavelength $\lambda$. Figure 9 highlights examples of reflectance spectra measured on clear days in July 2011.

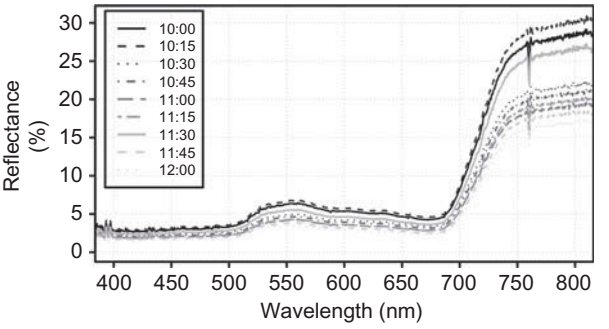


Figure 9. Reflectance spectra collected and processed between 10:00 and 12:00 (local time) on 6 July 2011 at the Hyytiälä field station, Finland.



Finally, we checked the stability of wavelength position regularly during the study period. Spectral calibrations were performed for both spectrometers by measuring the spectrum of an Ar-Hg lamp, in which Ar and Hg emit strongly at precisely known wavelengths. These lines are visible as peaks in the measured spectra, which are used to derive the centre position of each detector. Over the three spectral calibrations that we performed during the experiment, the maximum wavelength shifts of the peaks relative to the Ar-Hg lines were 0.12 nm at 546.07 nm for the reflected radiance spectrometer and 0.11 at 373.38 nm for the spectrometer measuring downwelling irradiance. The average wavelength shift for both instruments over all emission lines was 0.04 nm.

## 4. Discussion

In this paper we outline a newly developed, custom built, low-cost, low-power optical sampling system that meets the requirements for remote sensing of vegetation at narrow wavelengths and is highly applicable for both PRI and *F*. However, the extraction of wavelengths sensitive to a number of biophysical variables is possible given the detector coverage of the contiguous bands across the visible and near infrared. Overall the system differs from those developed to date for continuous operation, albeit few in number, through the incorporation of narrow band spectrometers, in combination with the modular nature of the system that would allow the user to swap the Ocean Optics spectrometers for spectrometers that are either broader or narrower in spectral resolution. These spectrometers are approximately 2.5k GBP, so compared with other spectrometers we regard these as very low cost, though for such operation considerable engineering for thermal stability is obviously critical.

The configuration of the system is such that the acquisition of the spectrometer with the shortest total acquisition time sits right in the middle of the total acquisition time of the other spectrometer. In practice, however, this is not exactly what happens, in part because of concurrent system threads running in the CPU but also because of the Normal triggering mode (free running) in which we chose to operate the spectrometers. When using this mode, the effective start times for both instruments will be shifted, forward or backward, by only a few milliseconds relative to their calculated start times. This is due to the fact that when in free-running mode, the spectrometers are continuously acquiring spectra and storing the last-measured spectrum in a buffer so that it is ready for the next trigger event (i.e. in our case this is the next start time). Therefore, if an acquisition is already ongoing at start time, it is the spectrum from that acquisition that will be delivered

as soon as the total acquisition duration (integration time × scans to average) finishes. The External Hardware triggering mode (not currently implemented in OO Controller) allows matching of the effective and calculated start times by triggering the spectrometers, which are kept on standby, with an excitation voltage (+5 V) on one of the USB2000+ 22 pins. This can be done, for example, using a USB-to-TTL cable interfaced with the controlling software. Also, additional delays caused by concurrent threads on the CPU could be eliminated by the OO Controller by prioritizing the spectrometer threads over other system threads using, for example, functions that implement the Real-Time Specification for Java (RTSJ).

During the first tests of the system on the outside, we had set the temperature controller set point at 30°C. We rapidly found that this set point did not dampen temperature diurnal variations sufficiently and resulted in unacceptable spectrometer temperature fluctuations. Further tests allowed us to choose 40°C as a set point that minimized the diurnal variations in spectrometer temperature to an acceptable level while still being within the instrument operating temperature range (−10 to +50°C). In testing different set point temperatures, we discovered that high temperatures have a significant effect on the analogue-to-digital controller of the USB2000+, which results in a decrease in measured intensity counts with increasing temperature. Factory baseline values in the spectrometers are adjusted for room temperature, but when operating the instrument at higher temperatures, this can result in the lowest intensity parts of the spectra recording a zero digital number. This has important consequences because, for spectrometers such as the USB2000+, those detectors that record the lowest intensities are the optically dark ones used for dark current corrections. Missing data in these detectors result in inability to calibrate raw spectra to absolute radiometric units, and users should pay close attention to this feature if operating the spectrometers at temperatures in excess of 35°C. This is, however, a solvable problem and after changing the baseline values to an adjusted operating temperature of 40–43°C using a program called USB EEPROM Programmer (www.oceanoptics.com/technical/usbprogrammer.pdf), a dark current reading was restored. Once thermal stability is reached, the system has proved to be very stable with respect to temperature and thus the calculated radiance, irradiance, and reflectance yielded quality outputs. As with many optical systems, and as highlighted in Balzarolo et al. (2011), regular calibrations are critical to ensure the highest data quality and to capture any changes or drift in the detectors. If the temperatures remain stable within the optics, monthly (or fewer) calibrations would be adequate. However, if there is any change in the operating temperature or if the system is in any way dismantled (i.e. fibres are detached from and reattached to the spectrometers) then a recalibration would be necessary. Further systems exist in the literature, though these are few in number. The reader is referred to the comprehensive review article by Balzarolo et al. (2011) for details on these. A feature of the current system is of course that there is no mechanism for cooling, only warming, so additional modifications that enable both heating and cooling would be essential in warmer climes. This was not an issue in boreal Finland, and the engineering was capable of coping with mid-summer temperatures, though this would not be the case in, for example, tropical environments, where cooling would be essential to maintain thermal stability.

## 5. Conclusions

We developed a new DFOV optical system capable of operating for extended periods (years). We assessed its reliability while operating it on an eddy covariance flux tower in Hyytiälä, Finland, from 2010 to the present. The possibility for future development of this

system exists insofar as replacement of the spectrometers with spectrometers of differing spectral resolution (e.g. the Ocean Optics HR4000) or other compact spectrometers depending on project requirements, without changing the other system components. Although we present a system based on a pair of spectrometers, the stable software platform developed in Java allows automation of multiple spectrometers with minimal input from an external party.

At the time of writing we have developed a new system capable of operation on board an aircraft and which operates to log irradiance in flight, for fusion with a high-resolution hyperspectral imager. Although not employed in the system here, it could be easily modified to include multi-angular sampling (e.g. following the Hilker AMSPEC system, Hilker et al. 2008) by adding rotating (e.g. step motor) or tilting (e.g. pan-tilt) hardware components.



## Acknowledgements

We are thankful to the EU Transnational Access programme via the University of Helsinki for supporting field-based accommodation at Hyytiala, Finland. We are indebted to Toivo Pahja and Veijo Hiltunen for overseeing and undertaking system checks during the project.

## Funding

This work was supported by the UK NERC under a Standard Grant [NE/F017294/1] to PI C.Nichol; the Academy of Finland Centre of Excellence programme project [1118615]; the Academy of Finland ICOS project [263149] and the EU ICOS project [211574].

## References

Adams III, W. W., K. Winter, U. Schreiber, and P. Schramel. 1990. "Photosynthesis and Chlorophyll Fluorescence Characteristics in Relationship to Changes in Pigment and Element Composition of Leaves of Platanus Occidentalis L. During Autumnal Leaf Senescence." *Plant Physiology* 93: 1184–1190.

Alonso, L., L. Gómez-Chova, J. Vila-Frances, J. Amoros-Lopez, L. Guanter, J. Calpe, and J. Moreno. 2008. "Improved Fraunhofer Line Discrimination Method for Vegetation Fluorescence Quantification." *IEEE Geoscience and Remote Sensing* 5 (4): 620–624.

Balzarolo, M., K. Anderson, C. J. Nichol, M. Rossini, L. Vescovo, N. Arriga, G. Wohlfahrt, J.-C. Calvet, A. Carrara, S. Cerasoli, S. Cogliati, F. Daumard, L. Eklundh, J. A. Elbers, F. Evrendilek, R. N. Handcock, J. Kaduk, K. Klumpp, B. Longdoz, G. Matteucci, M. Meroni, L. Montagnani, J.-M. Ourcival, E. P. Sánchez-Cañete, J.-Y. Pontailler, R. Juszczak, B. Scholes, and M. P. Martín. 2011. "Ground-Based Optical Measurements at European Flux Sites: A Review of Methods, Instruments and Current Controversies." *Sensors* 11 (9): 7954–7981.

Campbell, P. E. K., E. M. Middleton, L. A. Corp, and M. S. Kim. 2008. "Contribution of Chlorophyll Fluorescence to the Apparent Vegetation Reflectance." *Science of the Total Environment* 404: 433–439.

Campbell, P. E. K., E. M. Middleton, J. E. McMurtry, L. A. Corp, and E. W. Chappelle. 2007. "Assessment of Vegetation Stress Using Reflectance or Fluorescence Measurements." *Plant Environment Interactions* 36: 832–845.

Demmig-Adams, B. 1998. "Survey of Thermal Energy Dissipation and Pigment Composition in Sun and Shade Leaves." *Plant Cell Physiology* 39 (5): 474–482.

Demmig-Adams, B., and W. W. Adams III. 1996. "The Role of Xanthophyll Cycle Carotenoids in the Protection of Photosynthesis." *Trends in Plant Science* 1: 21–26.

Demmig-Adams, B., and W. W. Adams III. 2006. "Photoprotection in an Ecological Context: The Remarkable Complexity of Thermal Energy Dissipation." *New Phytologist* 172: 11–21.

Drolet, G., K. F. Huemmrich, F. G. Hall, E. M. Middleton, T. A. Black, A. G. Barr, and H. A. Margolis. 2005. "A MODIS-Derived Photochemical Reflectance Index to Detect Inter-Annual

Variations in the Photosynthetic Light-Use Efficiency of a Boreal Deciduous Forest." *Remote Sensing of Environment* 98: 212–224.

Drolet, G. G., E. M. Middleton, K. F. Huemmrich, F. G. Hall, B. D. Amiro, A. G. Barr, T. A. Black, J. H. McCaughey, and H. A. Margolis. 2008. "Regional Mapping of Gross Light-Use Efficiency Using MODIS Spectral Indices." *Remote Sensing of Environment* 112 (6): 3064–3078.

Frankenburg, C., C. O'Dell, L. Guanter, and J. McDuffie. 2012. "Chlorophyll Fluorescence Remote Sensing From Space in Scattering Atmospheres: Implications for its Retrieval and Interferences with Atmospheric $CO_2$ Retrievals." *Atmospheric Measurement Techniques Discussion* 5: 2487–2527.

Gamon, J. A., J. Peñuelas, and C. B. Field. 1992. "A Narrow-Waveband Spectral Index That Tracks Diurnal Changes in Photosynthetic Efficiency." *Remote Sensing of Environment* 41: 35–44.

Guanter, L., C. Frankenburg, A. Dudhia, P. E. Lewis, J. Gomez-Dans, A. Kuze, H. Suto, and R. G. Grainger. 2012. "Retrieval and Global Assessment of Terrestrial Chlorophyll Fluorescence from GOSAT Space Measurements." *Remote Sensing of Environment* 121: 236–251.

Hall, F. G., T. Hilker, and N. C. Coops. 2011. "PHOTOSYNSAT, Photosynthesis from Space: Theoretical Foundations of a Satellite Concept and Validation from Tower and Spaceborne Data." *Remote Sensing of Environment* 115: 1918–1925.

Hall, F. G., T. Hilker, N. C. Coops, A. Lyapustin, K. F. Huemmrich, E. M. Middleton, H. A. Margolis, G. Drolet, and T. A. Black. 2008. "Multi-Angle Remote Sensing of Forest Light Use Efficiency by Observing PRI Variation with Canopy Shadow Fraction." *Remote Sensing of Environment* 112: 3201–3211.

Hari, P., and N. Kulmala. 2005. "Station for Measuring Ecosystem-Atmosphere Relations." *Boreal Environment Research* 10: 315–322.

Hartmann, J., J. Fischer, U. Johannsen, and L. Werner. 2001. "Analytical Model for the Temperature Dependence of the Spectral Responsivity of Silicon." *Journal of Optical Society of America B* 18 (7): 942–947.

Hilker, T., N. C. Coops, F. G. Hall, T. A. Black, M. A. Wulder, Z. Nesic, and P. Krishnan. 2008. "Separating Physiologically and Directionally Induced Changes in PRI Using BRDF Models." *Remote Sensing of Environment* 112: 2777–2788.

Hilker, T., N. Coops, F. G. Hall, C. J. Nichol, A. Lyapustin, T. A. Black, M. A. Wulder, R. Leuning, A. Barr, D. Y. Hollinger, B. Munger, and C. J. Tucker. 2011. "Inferring Terrestrial Photosynthetic Light Use Efficiency of Temperate Ecosystems from Space." *Journal of Geophysical Research* 116: G03014. doi:10.1029/2011JG001692.

Hilker, T., N. C. Coops, Z. Nesic, M. A. Wulder, and T. A. Black. 2007. "Instrumentation and Approach for Unattended Year Round Tower Based Measurements of Spectral Reflectance." *Computers and Electronics in Agriculture* 56*:* 72–84.

Hilker, T., A. Lyapustin, F. G. Hall, Y. Wang, N. C. Coops, G. Drolet, and T. A. Black. 2009. "An Assessment of Photosynthetic Light Use Efficiency from Space: Modelling the Atmospheric and Directional Impacts on PRI Reflectance." *Remote Sensing of Environment* 113: 2463–2475.

IPCC. 2007. "Summary for Policymakers." In *Climate Change 2007: Impacts, Adaptation and Vulnerability. Contribution of Working Group II to the Fourth Assessment Report of the International Panel on Climate Change*, edited by M. L. Parry, O. F. Canziani, J. P. Palutikof, P. J. van der Linden, and C. E. Hanson, 7–22. Cambridge: Cambridge University Press.

Joiner, J., Y. Yoshida, A. P. Vasilkov, E. M. Middleton, P. E. K. Campbell, A. Kuze, and L. A. Corp. 2012. "Filling-in of Far-Red and Near-Infrared Solar Lines by Terrestrial and Atmospheric Effects: Simulations and Space Based Observations from SCHIAMACHY and GOSAT." *Atmospheric Measurement Techniques Discussion* 5 (1): 163–210.

Joiner, J., Y. Yoshida, A. P. Vasilkov, Y. Yoshida, L. A. Corp, and E. M. Middleton. 2011. "First Observations of Global and Seasonal Terrestrial Chlorophyll Fluorescence from Space." *Biogeosciences* 8: 637–651.

Linacre, E. 1992. *Climate Data and Resources: A Reference and Guide*. London: Routledge.

Logan, B. A., W. W. Adams III, and B. Demmig-Adams. 2007. "Avoiding Common Pitfalls of Chlorophyll Fluorescence Analysis under Field Conditions." *Functional Plant Biology* 34: 853–859.

Maier, S. W., K. P. Günther, and M. Stellmes. 2003. "Sun-Induced Fluorescence: A New Tool for Precision Farming." In *Digital Imaging and Spectral Techniques: Applications to Precision Agriculture and Crop Physiology*, edited by T. VanToai, D. Major, M. McDonald, J. Schepers, and L. Tarpley, 209–222. Madison, WI: American Society of Agronomy.

Meroni, M., and R. Colombo. 2006. "Leaf Level Detection of Solar Induced Chlorophyll Fluorescence by Means of a Subnanometer Resolution Spectroradiometer." *Remote Sensing of Environment* 103: 438–448.

Meroni, M., A. Barducci, S. Cogliati, F. Castagnoli, M. Rossini, L. Busetto, M. Migliavacca, E. Cremonese, M. Galvagno, R. Colombo, and U. Morra di Cella. 2011. "The Hyperspectral Irradiometer, a New Instrument for Long-Term and Unattended Field Spectroscopy Measurements." *Review of Scientific Instruments* 82 (4): 0431061–0431069.

Meroni, M., M. Rossini, L. Guanter, L. Alonso, U. Rascher, R. Colombo, and J. Moreno. 2009. "Remote Sensing of Solar-Induced Chlorophyll Fluorescence: Review of Methods and Applications." *Remote Sensing of Environment* 113: 2037–2051.

Moya, I., A. Ounis, N. Moise, and Y. Goulas. 2006. "First Airborne Multiwavelength Passive Chlorophyll Fluorescence Measurements over La Mancha (Spain) Fields." In *Second Recent Advances in Quantitative Remote Sensing*, edited by J. A. Sobrino, 820–825. Spain: Publicacions de la Universitat de València.

Plascyk, J. A. 1975. "The MK II Fraunhofer Line Discriminator (FLD-II) for Airborne and Orbital Remote Sensing of Solar-Stimulated Luminescence." *Optical Engineering* 14: 339–346.

Plascyk, J. A., and F. C. Gabriel. 1975. "The Fraunhofer Line Discriminator MKII – An Airborne Instrument for Precise and Standardized Ecological Luminescence Measurements." *IEEE Transations on Instrumentation and Measurements* 24: 306–313.

Porcar Castell, A., E. Juurola, I. Ensminger, F. Berninger, P. Hari, and E. Nikinmaa. 2008. "Seasonal Acclimation of Photosystem II in *Pinus Sylvestris*. II. Using the Rate Constants of Sustained Thermal Energy Dissipation and Photochemistry to Study the Effect of the Light Environment." *Tree Physiology* 28: 1483–1491.

Rollin, E. M., D. R. Emery, C. H. Kerr, and E. J. Milton. 1998. "Dual-Beam Reflectance Measurements and the Need for a Field Inter-Calibration Procedure." In *Developing International Connections. Proceedings of the 24th Annual Conference of the Remote Sensing Society*, 552–558. Nottingham: Remote Sensing Society.

Valentini, R., G. Matteucci, A. J. Dolman, E.-D. Schulze, C. Rebmann, E. J. Moors, A. Granier, P. Gross, N. O. Jensen, K. Pilegaard, A. Lindroth, A. Grelle, C. Bernhofer, T. Grünwald, M. Aubinet, R. Ceulemans, A. S. Kowalski, T. Vesala, U. Rannik, P. Berbigier, D. Loustau, J. Gudmundsson, H. Thorgeirsson, A. Ibrom, K. Morgenstern, R. Clement, J. Moncrieff, L. Montagnani, S. Minerbi, and P. G. Jarvis. 2000. "Respiration as the Main Determinant of Carbon Balance in European Forests." *Nature* 404: 861–865.